A Boundary Element Method for Molecular Electrostatics with Electrolyte Effects

Byung Jun Yoon and A. M. Lenhoff*

Department of Chemical Engineering, University of Delaware, Newark, Delaware 19716

Received 9 February 1990; accepted 7 May 1990

A boundary element method is developed to compute the electrostatic potential inside and around molecules in an electrolyte solution. A set of boundary integral equations are derived based on the integral formulations of the Poisson equation and the linearized Poisson–Boltzmann equation. The boundary integral equations are then solved numerically after discretizing the molecular surface into a number of flat triangular elements. The method is applied to a spherical molecule for which analytical solutions are available. Use is made of both constant and linearly varying unknowns over the boundary elements, and the method is tested for various values of parameters such as the dielectric constant of the molecule, ionic strength, and the location of the interior point charge. The use of the boundary integral method incorporating the nonlinear Poisson–Boltzmann equation is also briefly discussed.

INTRODUCTION

Electrostatic effects within biological macromolecules play an important role in determining their intramolecular structure and stability, while electrostatic interactions affect their intermolecular energetics and kinetics. Since the pioneering work of Kirkwood[1] several theoretical approaches have been developed for investigating electrostatic effects, in terms of the electrostatic potential and energy, of biomolecular systems. The electrostatics problems are commonly treated either microscopically or macroscopically. In the former the analysis is performed at an atomic level of detail, similar to that used in molecular dynamics simulations, whereas in the latter the biomolecule and the solvent are treated as two separate continuous media with different dielectric constants. Extensive reviews of various electrostatic models for biomolecules are available elsewhere.[2–5]

Because of its simplicity and the earlier success of the Tanford–Kirkwood theory,[6] which was based on a spherical cavity model with interior point charges, a continuum description has been favored by many research groups. In this model the molecular electrostatics are governed by the Poisson equation with different types of charge distributions for the interior and exterior regions of a molecule. For the interior region a volume distribution of point charges, originating from charged groups in amino acid residues (for proteins), is commonly used, while for the exterior region the number density of ionic species, considered as point charges, in the surrounding electrolyte solution is assumed to follow a Boltzmann distribution as in the Debye–Hückel theory of electrolytes.

The governing field equations, the Poisson equation and the Poisson–Boltzmann equation, may be solved using various methods, either analytical or numerical. Since the Poisson–Boltzmann equation is nonlinear, analytical approaches are possible only after linearization of the equation, commonly referred to as the Debye–Hückel approximation. The Poisson equation and the linearized Poisson–Boltzmann equation, which is similar to the Helmholtz equation, are separable in several orthogonal coordinate systems,[7] so analytical solutions can be obtained for simple bodies such as spheres.[1]

However, for biomolecules of complicated shape, especially for those whose three-dimensional crystal structure has been resolved, the governing field equations can be solved only by numerical methods. One may adopt either a domain method or a boundary method for this purpose. In the former the entire domain, both molecule and solvent, is discretized, and the potential at each nodal point is determined. The finite difference method[8] and the finite element method[9] belong in this category. The earliest versions of these methods considered only the Poisson equation, without the effects of ionic strength. Further development of the finite difference approach has been achieved by including the linearized Poisson–Boltzmann equation,[10,11]

*To whom all correspondence should be addressed.

Journal of Computational Chemistry, Vol. 11, No. 9, 1080–1086 (1990)

CCC 0192-8651/90/0901080-07$04.00

and the nonlinear Poisson–Boltzmann equation[12] in the analysis.

In contrast with the domain method, the boundary method is based on an integral formulation of the governing equations. Thus, one needs to solve numerically the integral equations, for which a discretization of only the boundary surface is usually required. With a view to applications to biomolecules the boundary method, commonly referred to as the boundary element method, has several advantages as compared with the finite difference method. First, a discretization of the surface rather than the whole domain of interest reduces the dimensionality of the problem by one, thus greatly reducing the size of the set of algebraic equations to be solved. Second, one can easily treat infinite or semi-infinite domains without the need for a large artificial boundary which contains the domain of interest. Third, one can place interior point charges at their exact locations without resorting to an artificial distribution of fractional charges onto neighboring grid points.[13,14]

The boundary element method has been widely applied to potential problems since the 1960s. There are two approaches to formulating the boundary element method based on the type of integral equation used, namely the indirect method and the direct method. In the former the solution is expressed as a surface integral of either the single-layer potential or the double-layer potential with unknown surface density, while in the latter the governing partial differential equation is reformulated as an integral equation utilizing Green's identity. Advantages and disadvantages of both approaches are discussed elsewhere.[15,16] Previous applications of the boundary element method to molecular electrostatics[17–20] have generally been limited to the case of zero ionic strength, for which the indirect method has invariably been used; this is a convenient choice since both interior and exterior potentials can be expressed in terms of the single Green function. However, with electrolyte effects the indirect method cannot describe the exterior potential in terms of the single-layer potential only, but instead requires an additional volume potential term which contributes to the surface density of the single-layer potential. For this purpose Rashin[21] has suggested an iterative scheme, which is commonly used for nonlinear problems.[15]

The aim of this work is to develop a direct boundary element method utilizing the integral representations of the Poisson equation and the linearized Poisson–Boltzmann equation. We test the method on model problems involving spherical molecules in various situations, for which analytical solutions are available. We also discuss the extension of the method to include the nonlinear Poisson–Boltzmann equation.

INTEGRAL FORMULATION

Consider a molecule in an electrolyte solution, with the interior and exterior regions of the molecule denoted by B^i and B^e respectively. Throughout this work the superscripts i, e, and s are used to denote the interior, exterior, and surface of the molecule, respectively. The interior potential ϕ^i and the exterior potential ϕ^e are governed by the Poisson equation

$$\nabla^2\phi^i(\mathbf{x}) = -\frac{1}{\epsilon^i}\sum_{k=1}^{n} q_k\,\delta(\mathbf{x}-\mathbf{x}_k) \quad \text{for } \mathbf{x}\in B^i \tag{1}$$

and the linearized Poisson–Boltzmann equation

$$\nabla^2\phi^e(\mathbf{x}) = \kappa^2\phi^e(\mathbf{x}) \quad \text{for } \mathbf{x}\in B^e, \tag{2}$$

respectively. Here ϵ^i denotes the uniform dielectric constant of the molecule and $\delta(\mathbf{x})$ is the three-dimensional delta function. Inside the molecule a set of n point charges q_k are placed at positions $\mathbf{x}_k$. The linearization of the Poisson–Boltzmann equation is a result of the Debye–Hückel approximation applicable in the case of low potentials with the Debye length $1/\kappa$ characterizing the screening effect due to the surrounding electrolyte. The boundary conditions at the molecular surface ∂B are

$$\phi^i = \phi^e \quad \text{and} \quad \epsilon^i\frac{\partial\phi^i}{\partial n} = \epsilon^e\frac{\partial\phi^e}{\partial n} \tag{3a, b}$$

the continuity of the potential and the normal component of the electric displacement respectively. Here $\mathbf{n}$ denotes the outward unit normal vector to the molecular surface and ϵ^e is the dielectric constant of the electrolyte solution.

An integral formulation of the Poisson eq. (1) is most readily obtained using Green's second identity.[22,23] The resulting integral equation, also known as Green's third identity, for the interior potential is given by

$$\begin{aligned}\phi^i(\mathbf{x}) = {} & \frac{1}{4\pi}\sum_{k=1}^{n}\frac{q_k}{\epsilon^i|\mathbf{x}-\mathbf{x}_k|} + \frac{1}{4\pi} \\ & \times\int_{\partial B}\frac{\partial\phi^i}{\partial n}\frac{1}{|\mathbf{x}-\mathbf{x}'|}\,dA(\mathbf{x}') - \frac{1}{4\pi} \\ & \times\int_{\partial B}\phi^i\frac{\partial}{\partial n}\left(\frac{1}{|\mathbf{x}-\mathbf{x}'|}\right)dA(\mathbf{x}') \\ & \text{for } \mathbf{x}\in B^i\end{aligned} \tag{4}$$

In addition to the potential contributed by interior point charges, the potentials of the surface distributions of point charges and point dipoles contribute to the total interior potential. The first surface integral is called the single-layer potential, while the second surface integral is called the double-layer potential. In order to compute the potential at arbitrary interior

points we need to know the densities of the single and double layers, i.e., the normal derivative of the potential on the surface and the surface potential respectively.

The corresponding integral formulation of the linearized Poisson–Boltzmann eq. (2) is given by

$$\phi^e(\mathbf{x}) = -\frac{1}{4\pi}\int_{\partial B}\frac{\partial\phi^e}{\partial n}\frac{\exp(-\kappa|\mathbf{x}-\mathbf{x}'|)}{|\mathbf{x}-\mathbf{x}'|}dA(\mathbf{x}') + \frac{1}{4\pi}\int_{\partial B}\phi^e\frac{\partial}{\partial n}\left(\frac{\exp(-\kappa|\mathbf{x}-\mathbf{x}'|)}{|\mathbf{x}-\mathbf{x}'|}\right) \times dA(\mathbf{x}') \quad \text{for } \mathbf{x}\in B^e \tag{5}$$

The single-layer potential consists of point charges with screening, the Green function of the linearized Poisson–Boltzmann equation. In order to match the potential fields (4)–(5) at the boundary we need the corresponding integral equations when $\mathbf{x}\in\partial B$. Utilizing the jump discontinuity of the double-layer potential at the boundary, we can obtain the following integral equations when $\mathbf{x}^s\in\partial B$.

$$\frac{1}{2}\phi^i(\mathbf{x}^s) = \frac{1}{4\pi}\sum_{k=1}^{n}\frac{q_k}{\epsilon^i|\mathbf{x}^s-\mathbf{x}_k|} + \frac{1}{4\pi}\int_{\partial B}\frac{\partial\phi^i}{\partial n}\times\frac{1}{|\mathbf{x}^s-\mathbf{x}'|}dA(\mathbf{x}') - \frac{1}{4\pi}\int_{\partial B}\phi^i\frac{\partial}{\partial n}\times\left(\frac{1}{|\mathbf{x}^s-\mathbf{x}'|}\right)dA(\mathbf{x}'), \tag{6}$$

$$\frac{1}{2}\phi^e(\mathbf{x}^s) = -\frac{1}{4\pi}\int_{\partial B}\frac{\partial\phi^e}{\partial n}\frac{\exp(-\kappa|\mathbf{x}^s-\mathbf{x}'|)}{|\mathbf{x}^s-\mathbf{x}'|}dA(\mathbf{x}') + \frac{1}{4\pi}\int_{\partial B}\phi^e\frac{\partial}{\partial n}\left(\frac{\exp(-\kappa|\mathbf{x}^s-\mathbf{x}'|)}{|\mathbf{x}^s-\mathbf{x}'|}\right)\times dA(\mathbf{x}'). \tag{7}$$

After using the boundary conditions (3a, b) we finally obtain a set of two boundary integral equations:

$$\phi^s(\mathbf{x}^s) = \frac{1}{2\pi}\sum_{k=1}^{n}\frac{q_k}{\epsilon^i|\mathbf{x}^s-\mathbf{x}_k|} + \frac{1}{2\pi}\frac{\epsilon^e}{\epsilon^i}\int_{\partial B}\frac{\partial\phi^e}{\partial n}\times\frac{1}{|\mathbf{x}^s-\mathbf{x}'|}dA(\mathbf{x}') - \frac{1}{2\pi}\int_{\partial B}\phi^s\frac{\partial}{\partial n}\times\left(\frac{1}{|\mathbf{x}^s-\mathbf{x}'|}\right)dA(\mathbf{x}'), \tag{8}$$

$$\phi^s(\mathbf{x}^s) = -\frac{1}{2\pi}\int_{\partial B}\frac{\partial\phi^e}{\partial n}\frac{\exp(-\kappa|\mathbf{x}^s-\mathbf{x}'|)}{|\mathbf{x}^s-\mathbf{x}'|}dA(\mathbf{x}') + \frac{1}{2\pi}\int_{\partial B}\phi^s\frac{\partial}{\partial n}\left(\frac{\exp(-\kappa|\mathbf{x}^s-\mathbf{x}'|)}{|\mathbf{x}^s-\mathbf{x}'|}\right)\times dA(\mathbf{x}'). \tag{9}$$

Here the unknowns are the surface potential ϕ^s and its exterior normal derivative $\partial\phi^e/\partial n$. After solving eqs. (8)–(9) one can compute the potential at any arbitrary points using (4)–(5).

SIMPLE EXAMPLE

In general the boundary integral eqs. (8)–(9) must be solved numerically. However, in this section we consider a simple example for which the solution can be obtained analytically. Consider a spherical molecule of radius R with a single point charge q located at the center. Because of the symmetry, ϕ^s and $\partial\phi^e/\partial n$ are independent of angular position. In order to solve the boundary integral eqs. (8)–(9) we need to evaluate four surface integrals, which are given by

$$\int_{\partial B}\frac{1}{|\mathbf{x}^s-\mathbf{x}'|}dA(\mathbf{x}') = 4\pi R,$$

$$\int_{\partial B}\frac{\partial}{\partial n}\frac{1}{|\mathbf{x}^s-\mathbf{x}'|}dA(\mathbf{x}') = -2\pi,$$

$$\int_{\partial B}\frac{\exp(-\kappa|\mathbf{x}^s-\mathbf{x}'|)}{|\mathbf{x}^s-\mathbf{x}'|}dA(\mathbf{x}') = \frac{2\pi}{\kappa}\times[1-\exp(-2\kappa R)],$$

$$\int_{\partial B}\frac{\partial}{\partial n}\left(\frac{\exp(-\kappa|\mathbf{x}^s-\mathbf{x}'|)}{|\mathbf{x}^s-\mathbf{x}'|}\right)dA(\mathbf{x}') = -\frac{2\pi}{\kappa R}\times[-\exp(-2\kappa R)-\kappa R\exp(-2\kappa R)].$$

The corresponding solutions of the boundary integral equations are then given by

$$\phi^s = \frac{q}{4\pi\epsilon^e R(1+\kappa R)},$$

$$\frac{\partial\phi^e}{\partial n} = -\frac{q}{4\pi\epsilon^e R^2}.$$

Substituting these surface values into (4)–(5), we can determine the interior and exterior potential fields:

$$\phi^i = \frac{q}{4\pi\epsilon^i r} - \frac{q}{4\pi\epsilon^i R} + \frac{q}{4\pi\epsilon^e(1+\kappa R)R},$$

$$\phi^e = \frac{q\exp(-\kappa(r-R))}{4\pi\epsilon^e(1+\kappa R)r}.$$

Here r denotes the radial distance from the sphere center. The same solutions can be readily obtained directly by solving the original differential eqs. (1)–(2) in spherical coordinates.

NUMERICAL SOLUTION

In order to solve the boundary integral eqs. (8)–(9) in more complex situations, we first discretize the molecular surface into a number of small boundary elements, either flat or curved. Triangular and quadrilateral elements are commonly used for this purpose. We then assume an appropriate

functional form of the unknowns, ϕ^s and $\partial\phi^e/\partial n$, over each boundary element. Consider N boundary elements and use the symbols v and w for ϕ^s and $\partial\phi^e/\partial n$, respectively. The value of v_i at $\mathbf{x}_i \in \partial B$ $(i = 1,\ldots,M)$ is then given from (8)–(9) by

$$v_i(\mathbf{x}_i) = \frac{1}{2\pi}\sum_{k=1}^{n}\frac{q_k}{\epsilon^i|\mathbf{x}_i - \mathbf{x}_k|} + \frac{1}{2\pi}\frac{\epsilon^e}{\epsilon^i}\sum_{j=1}^{N}\int_j w(\mathbf{x}')\frac{1}{|\mathbf{x}_i - \mathbf{x}'|}\,dA_j(\mathbf{x}') - \frac{1}{2\pi}\sum_{j=1}^{N}\int_j v(\mathbf{x}')\frac{\partial}{\partial n}\left(\frac{1}{|\mathbf{x}_i - \mathbf{x}'|}\right)dA_j(\mathbf{x}'), \tag{10}$$

$$v_i(\mathbf{x}_i) = -\frac{1}{2\pi}\sum_{j=1}^{N}\int_j w(\mathbf{x}')\frac{\exp(-\kappa|\mathbf{x}_i - \mathbf{x}'|)}{|\mathbf{x}_i - \mathbf{x}'|}dA_j(\mathbf{x}') + \frac{1}{2\pi}\sum_{j=1}^{N}\int_j v(\mathbf{x}')\frac{\partial}{\partial n}\left(\frac{\exp(-\kappa|\mathbf{x}_i - \mathbf{x}'|)}{|\mathbf{x}_i - \mathbf{x}'|}\right)dA_j(\mathbf{x}') \tag{11}$$

This set of $2M$ linear algebraic equations are the final equations to be solved.

We test our method on a spherical model molecule with an arbitrary internal charge distribution, for which an analytical solution is available.[1] Flat triangular elements are used. Figure 1 shows a triangulated surface composed of 720 elements. For the functional forms of v and w over a boundary element, two types are studied: constant and linear cases. In the former constant values are assumed for v and w for each element, and $\mathbf{x}_i$'s are chosen at the centroids of elements, so that $M = N$ (720 for Figure 1). The first surface integral in (10) then reduces to

$$\int_j w(\mathbf{x}')\frac{1}{|\mathbf{x}_i - \mathbf{x}'|}\,dA_j(\mathbf{x}') = w_j\int_j \frac{1}{|\mathbf{x}_i - \mathbf{x}'|}\,dA_j(\mathbf{x}'),$$

where w_j is the value of w on the jth element. Other integrals appear in similar forms. On the other hand, the linear case assumes linear variations in v and w on each element, and $\mathbf{x}_i$'s are chosen at the vertices of elements, so that $M =$ the number of nodes (362 for Figure 1). The first integral in (10) now reduces to

$$\int_j w(\mathbf{x}')\frac{1}{|\mathbf{x}_i - \mathbf{x}'|}\,dA_j(\mathbf{x}') = \int_j \frac{w_{j1}\alpha(\mathbf{x}') + w_{j2}\beta(\mathbf{x}') + w_{j3}\gamma(\mathbf{x}')}{|\mathbf{x}_i - \mathbf{x}'|}\,dA_j(\mathbf{x}'),$$

where w_{jk}'s are the values of w at the three vertices of the jth element. Here α, β, and γ are area coordinates of a triangle, defined by

$$\begin{pmatrix} x' \\ y' \\ z' \end{pmatrix} = \begin{pmatrix} x_1 & x_2 & x_3 \\ y_1 & y_2 & y_3 \\ z_1 & z_2 & z_3 \end{pmatrix}\begin{pmatrix} \alpha \\ \beta \\ \gamma \end{pmatrix}.$$

In our computations the integrals in (10)–(11) are evaluated using a six-point Gaussian quadrature formula, except for $\mathbf{x}_i \in dA_j$, where the integrals are evaluated analytically.

NUMERICAL RESULTS

We choose to compute the potential fields inside and around a spherical molecule of 15 Å radius

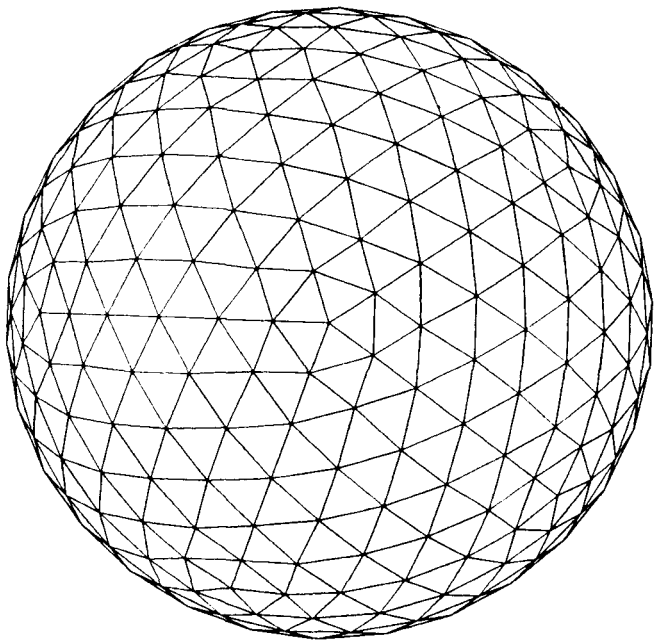

Figure 1. Surface discretization of a spherical molecule into 720 flat triangular elements.

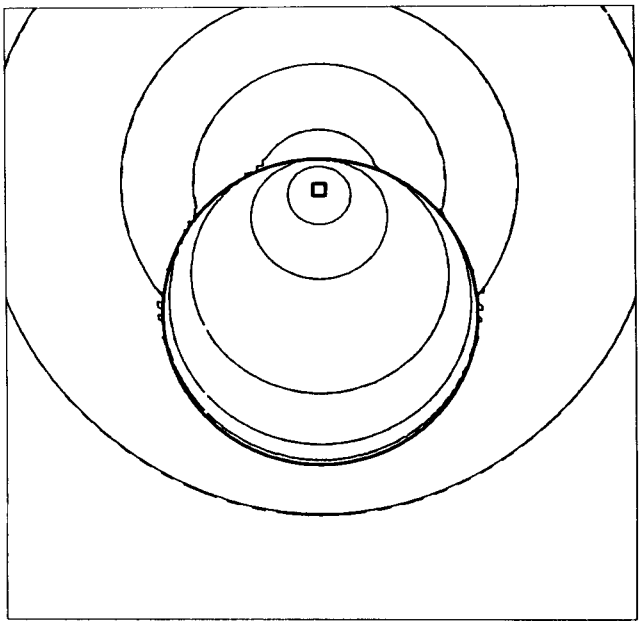

Figure 2. Equipotential contours for a spherical molecule of radius 15 Å. Both numerical (solid line) and analytical (broken line) results are shown along with the location of unit positive charge at radius 12 Å. Equipotentials are plotted in units of kT/e (0.005, 0.05, 0.2, 1.0, 10.0, and 50.0 are shown) at room temperature. Other parameters are: $1/\kappa$ = 7.5 Å, ϵ^i = 2, ϵ^e = 80.

with dielectric constant 2. The electrolyte solution, with dielectric constant 80, is at physiological conditions, for which the corresponding Debye length $1/\kappa$ is 7.5 Å. A unit positive charge is placed at radius 12 Å. Figure 2 shows equipotential contours from both numerical and analytical results. Potentials are plotted in units of kT/e, where kT is the Boltzmann energy and e is the elementary charge. In this example 720 elements are used with linear variation of unknowns over each element. Agreement is very good, with the numerical and analytical results almost identical.

In order to investigate the advantages of the use of linear basis functions compared with that of constant basis functions, we plot in Figure 3 relative % errors of numerically computed potentials as a function of dimensionless distance, normalized to the sphere radius, from the center along the line passing through the point charge. The point charge is located at radius 12 Å as in the previous example and the same physical conditions are used. Four cases are investigated: constant and linear 320-element cases, and constant and linear 720-element cases. The linear versions generally produce more accurate results than the constant versions. Since the linear version produces fewer unknowns than the constant version for the same number of elements, it also requires less computing time. Computing times on a VAX 11/785 are: constant 320-element, 15 min; linear 320-element, 3 min; constant 720-element, 2 h 7 min; linear 720-element, 28 min. Therefore, in terms of both accuracy and economy, the linear versions are superior to the constant versions. All subsequent examples presented in this section are based on the linear 720-element version.

From Figure 3 we can note that the maximum relative error is observed at the surface, while the relative error reaches its minimum near the location of the point charge. This trend is quite different from that in the results of the finite difference method, in which the maximum error is observed near the location of the point charge. Since the potential field near the point charge is influenced mainly by the point charge itself, and since this contribution is explicitly included in (4), the

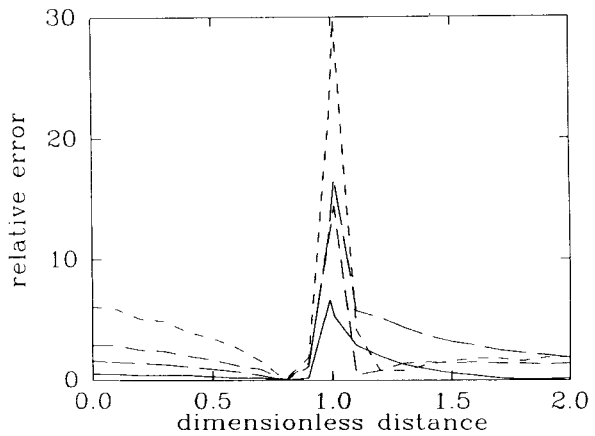

Figure 3. Relative % errors for potentials as a function of dimensionless distance from the center. Key: ---- constant 320-element; – – – constant 720-element; — — linear 320-element; —— linear 720-element.

boundary element method furnishes a more accurate potential field near the point charge. Unfortunately, the trends near the surface can not be compared since the exact location of the boundary surface is not clearly defined in the finite difference method.

Despite some controversy over the dielectric constant of proteins, as a consensus a dielectric constant in the range of 2–4 is generally used.[24] Figure 4 shows the effect of the dielectric constant ϵ^i on the relative errors. Three different values are considered: 1, 2, and 4. As expected, errors decrease as the interior dielectric constant increases, since the difference between the interior dielectric constant and the exterior dielectric constant, which is set at 80, becomes smaller. In general, however, the performance of the boundary element method is not affected significantly by the change in the interior dielectric constant.

The effects of ionic strength are shown in Figure 5 in terms of the relative errors in potentials for various values of the Debye length: 3 Å, 7.5 Å, and 18.75 Å. The interior potentials as well as the surface potentials are hardly affected, but the exterior potentials become less accurate as the ionic strength increases. As the Debye length decreases, the relevant length scale of the exterior potential field also decreases. Thus in order to retain the same level of resolution one needs a finer discretization of the surface.

Finally we consider the effects of the location of the point charge, one of the most important issues in the performance of any numerical method. Intuitively one can expect larger errors in potentials as the point charge approaches the boundary surface, unless one uses finer surface elements. Figure 6 shows the relative errors in potentials for the cases of the point charge at radii 12 Å and 13.5 Å. Even at 13.5 Å the maximum error remains less than 10%, and the accuracy of the exterior potentials does not deteriorate significantly. Note that the size of a surface triangle of the 720-element sphere is about 2.5 Å. Thus, when the point charge is near the boundary surface, i.e., much closer than the linear dimension of adjacent surface elements, it is advisable to use correspondingly finer surface elements.

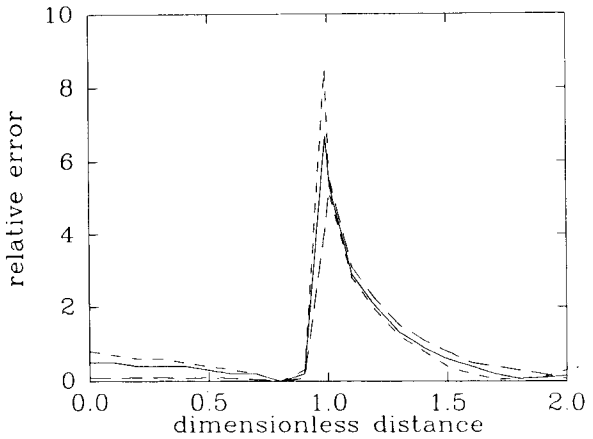

Figure 4. Relative % errors for potentials as a function of dimensionless distance from the center. Key: ---- $\epsilon^i = 1$; —— $\epsilon^i = 2$; — — — $\epsilon^i = 4$.

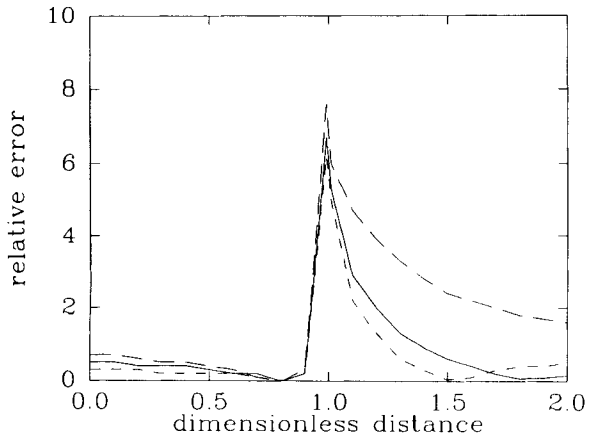

Figure 5. Relative % errors for potentials as a function of dimensionless distance from the center. Key: ---- $1/\kappa$ = 18.75 Å; —— $1/\kappa$ = 7.5 Å; — — — $1/\kappa$ = 3 Å.

DISCUSSION AND CONCLUSIONS

We have developed a boundary element method suitable for biomolecular electrostatics computations. Compared to the earlier method, the so-called surface polarization charge method, our method effectively takes account of electrolyte effects by simultaneously solving both the Poisson equation and the linearized Poisson–Boltzmann equation at the boundary surface. Test results for a spherical molecule are in good agreement with the corresponding analytical results over a range of physical conditions, and the method can be readily applied to electrostatics computations for

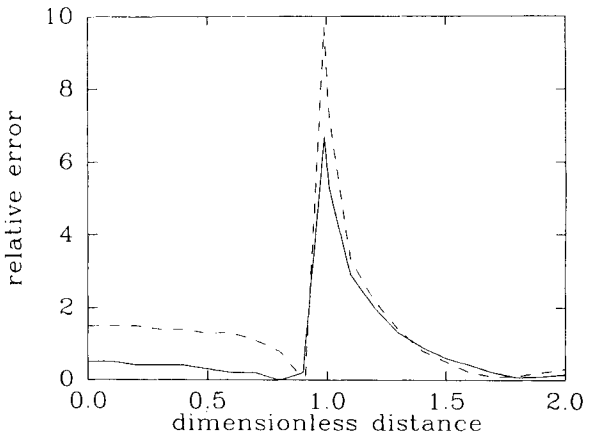

Figure 6. Relative % errors for potentials as a function of dimensionless distance from the center. The solid line is for the point charge at radius 12 Å, while the broken line is for the point charge at radius 13.5 Å.

biomolecules of which the crystal structures are available. The surface triangulation algorithm developed by Connolly[25] can, for instance, be used for this purpose.

In this work we used a linearized version of the Poisson–Boltzmann equation to describe the exterior potential field. The linearization is valid only when the potentials are small, i.e., when $\phi^e \ll kT/e$. However, as can be seen in Figure 2, this condition is not strictly satisfied, especially in the region near the point charge. In order to incorporate the nonlinear Poisson–Boltzmann equation in the boundary element method, one must derive the corresponding integral representation of the equation. For the sake of simplicity, consider a 1:1 electrolyte solution. The Poisson–Boltzmann equation, in terms of the dimensionless potential, can be recast to

$$(\nabla^2 - \kappa^2)\phi^e(\mathbf{x}) = \kappa^2 \sinh \phi^e(\mathbf{x}) - \kappa^2\phi^e(\mathbf{x}) \quad \text{for } \mathbf{x} \in B^e. \tag{2'}$$

We may consider this equation as the linearized Poisson–Boltzmann equation with an additional volume charge density, and utilizing Green's second identity we can obtain the following integral formulation:

$$\phi^e(\mathbf{x}) = -\frac{1}{4\pi}\int_{B^e} \frac{\kappa^2 \sinh \phi^e(\mathbf{x}') - \kappa^2\phi^e(\mathbf{x}')}{|\mathbf{x} - \mathbf{x}'|}\, dV(\mathbf{x}') - \frac{1}{4\pi}\int_{\partial B} \frac{\partial\phi^e}{\partial n}\frac{\exp(-\kappa|\mathbf{x} - \mathbf{x}'|)}{|\mathbf{x} - \mathbf{x}'|}\, dA(\mathbf{x}') + \frac{1}{4\pi}\int_{\partial B} \phi^e \frac{\partial}{\partial n}\left(\frac{\exp(-\kappa|\mathbf{x} - \mathbf{x}'|)}{|\mathbf{x} - \mathbf{x}'|}\right) dA(\mathbf{x}'). \tag{5'}$$

The corresponding boundary integral equation is given by

$$\phi^s(\mathbf{x}^s) = -\frac{1}{2\pi}\int_{B^e} \frac{\kappa^2 \sinh \phi^e(\mathbf{x}') - \kappa^2\phi^e(\mathbf{x}')}{|\mathbf{x}^s - \mathbf{x}'|}\, dV(\mathbf{x}') - \frac{1}{2\pi}\int_{\partial B} \frac{\partial\phi^e}{\partial n}\frac{\exp(-\kappa|\mathbf{x}^s - \mathbf{x}'|)}{|\mathbf{x}^s - \mathbf{x}'|}\, dA(\mathbf{x}') + \frac{1}{2\pi}\int_{\partial B} \phi^e \frac{\partial}{\partial n}\left(\frac{\exp(-\kappa|\mathbf{x}^s - \mathbf{x}'|)}{|\mathbf{x}^s - \mathbf{x}'|}\right) dA(\mathbf{x}'). \tag{9'}$$

Since the density of this new volume potential is unknown, one has to resort to iterative methods to solve the boundary integral eqs. (8) and (9'). For instance, one can start with the ϕ^e determined from the linearized Poisson–Boltzmann equation, as in the previous section. The volume integral in (9') can then be computed numerically after a proper discretization of the exterior region. After substituting this value into eq. (9'), one can solve the boundary integral eqs. (8) and (9'). The solution of the boundary integral equations and the initial set of ϕ^e values are then used to determine the second set of ϕ^e values using (5'). Iteration is continued until an appropriate convergence condition is satisfied. Although evaluation of the volume integral is somewhat cumbersome, this method will be valuable in determining the validity of the use of the linearized Poisson–Boltzmann equation in biomolecular electrostatics computations.

We thank Mr. Yuris O. Fuentes of the University of Wisconsin-Madison for providing the tesselation algorithm for spheres. This work was supported by the National Science Foundation through Grant CTS-8657185.

References

1. J. G. Kirkwood, *J. Chem. Phys.*, **2,** 351 (1934).
2. S. C. Harvey, *Proteins,* **5,** 78 (1989).
3. J. B. Matthew, *Ann. Rev. Biophys. Biophys. Chem.,* **14,** 387 (1985).
4. N. K. Rogers, *Prog. Biophys. Molec. Biol.,* **48,** 37 (1986).
5. A. Warshel and S. T. Russell, *Quart. Rev. Biophys.,* **17,** 283 (1984).
6. C. Tanford and J. G. Kirkwood, *J. Am. Chem. Soc.,* **79,** 5333 (1957).
7. P. M. Morse and H. Feshbach, *Methods of Theoretical Physics,* McGraw-Hill, New York, 1953.
8. J. Warwicker and H. C. Watson, *J. Mol. Biol.,* **157,** 671 (1982).
9. W. H. Orttung, *Ann. N.Y. Acad. Sci.,* **303,** 22 (1977).
10. I. Klapper, R. Hagstrom, R. Fine, K. Sharp, and B. Honig, *Proteins,* **1,** 47 (1986).
11. J. Warwicker, *J. Theor. Biol.,* **121,** 199 (1986).
12. B. Jayaram, K. A. Sharp, and B. Honig, *Biopolymers,* **28,** 975 (1989).
13. M. K. Gilson, K. A. Sharp, and B. H. Honig, *J. Comp. Chem.,* **9,** 327 (1987).
14. N. K. Rogers and M. J. E. Sternberg, *J. Mol. Biol.,* **174,** 527 (1984).
15. D. E. Beskos, *Boundary Element Methods in Mechanics,* North-Holland, Amsterdam, 1987.
16. M. A. Jaswon and G. T. Symm, *Integral Equation Methods in Potential Theory and Elastostatics,* Academic Press, New York, 1977.
17. S. Miertus, E. Scrocco, and J. Tomasi, *Chem. Phys.,* **55,** 117 (1981).
18. A. A. Rashin and K. Namboodiri, *J. Phys. Chem.,* **91,** 6003 (1987).
19. R. J. Zauhar and R. S. Morgan, *J. Mol. Biol.,* **186,** 815 (1985).
20. R. J. Zauhar and R. S. Morgan, *J. Comp. Chem.,* **9,** 171 (1988).
21. A. A. Rashin, *J. Phys. Chem.,* **94,** 1725 (1990).
22. J. D. Jackson, *Classical Electrodynamics,* 2nd Ed., Wiley, New York, 1975.
23. O. D. Kellogg, *Foundations of Potential Theory,* Dover, New York, 1953.
24. M. K. Gilson and B. H. Honig, *Biopolymers,* **25,** 2097 (1986).
25. M. L. Connolly, *J. Appl. Cryst.,* **18,** 499 (1985).